The EMBO Journal (2011) 30, 130–144 | © 2011 European Molecular Biology Organization | All Rights Reserved 0261-4189/11
www.embojournal.org

THE EMBO JOURNAL

CAMP (C13orf8, ZNF828) is a novel regulator of kinetochore–microtubule attachment

Go Itoh[1], Shin-ichiro Kanno[2], Kazuhiko SK Uchida[3], Shuhei Chiba[4], Shiro Sugino[1], Kana Watanabe[1], Kensaku Mizuno[4], Akira Yasui[2], Toru Hirota[3] and Kozo Tanaka[1,*]

[1]Institute of Development, Aging and Cancer, Tohoku University, Miyagi, Japan, [2]Division of Dynamic Proteome in Aging and Cancer, Institute of Development, Aging and Cancer, Tohoku University, Miyagi, Japan, [3]Division of Experimental Pathology, Cancer Institute, Japanese Foundation for Cancer Research, Tokyo, Japan and [4]Department of Biomolecular Sciences, Graduate School of Life Sciences, Tohoku University, Miyagi, Japan

Proper attachment of microtubules to kinetochores is essential for accurate chromosome segregation. Here, we report a novel protein involved in kinetochore–microtubule attachment, chromosome alignment-maintaining phosphoprotein (CAMP) (C13orf8, ZNF828). CAMP is a zinc-finger protein containing three characteristic repeat motifs termed the WK, SPE, and FPE motifs. CAMP localizes to chromosomes and the spindle including kinetochores, and undergoes CDK1-dependent phosphorylation at multiple sites during mitosis. CAMP-depleted cells showed severe chromosome misalignment, which was associated with the poor resistance of K-fibres to the tension exerted upon establishment of sister kinetochore bi-orientation. We found that the FPE region, which is responsible for spindle and kinetochore localization, is essential for proper chromosome alignment. The C-terminal region containing the zinc-finger domains negatively regulates chromosome alignment, and phosphorylation in the FPE region counteracts this regulation. Kinetochore localization of CENP-E and CENP-F was affected by CAMP depletion, and by expressing CAMP mutants that cannot functionally rescue CAMP depletion, placing CENP-E and CENP-F as downstream effectors of CAMP. These data suggest that CAMP is required for maintaining kinetochore–microtubule attachment during bi-orientation.

The EMBO Journal (2011) **30,** 130–144. doi:10.1038/emboj.2010.276; Published online 9 November 2010
Subject Categories: cell cycle
Keywords: chromosome; kinetochore; metaphase; microtubule; spindle

Introduction

For accurate chromosome segregation, attachment of sister kinetochores on a replicated chromosome to microtubules from opposite spindle poles (bi-orientation) must be achieved (Tanaka *et al*, 2005; Tanaka, 2008; Walczak *et al*, 2010). Thus far, a number of molecules have been identified that are essential for accurate chromosome segregation, including molecules directly involved in kinetochore–microtubule attachment (Cheeseman *et al*, 2006; Cheeseman and Desai, 2008; Tanaka and Desai, 2008) and the correction of erroneous attachments (Ruchaud *et al*, 2007), as well as components of the spindle assembly checkpoint (SAC) that prevents anaphase onset until proper kinetochore–microtubule attachment to all chromosomes has been achieved (Musacchio and Salmon, 2007). Many of these molecules are conserved from yeast to human, but some are found specifically in mammalian cells where they are suggested to be involved in the precise regulation of mammalian kinetochore–microtubule attachment. Identification of such molecules will not only allow us to further understand the control of chromosome segregation in human cells, but could also have clinical significance, as dysregulation of chromosome segregation may lead to oncogenic transformation through the induction of chromosomal instability (Weaver and Cleveland, 2005; Ganem *et al*, 2007; Ricke *et al*, 2008; Tanaka and Hirota, 2009).

Here, we report a novel regulator for accurate chromosome segregation, chromosome alignment-maintaining phosphoprotein (CAMP). We identified CAMP as a MAD2L2-interacting protein. MAD2L2, together with MAD2L1, is an orthologue of yeast MAD2 that has a central function in the SAC (Cahill *et al*, 1999). While MAD2L1 is the canonical MAD2, MAD2L2 shares homology with yeast REV7, a component of polymerase ζ (pol ζ), which is involved in translesion synthesis (Gan *et al*, 2008). In contrast to MAD2L1, which inhibits activation of the anaphase-promoting complex/cyclosome (APC/C) through its interaction with CDC20 (Musacchio and Salmon, 2007), MAD2L2 inhibits APC/C through binding with another APC/C cofactor, CDH1 (Chen and Fang, 2001; Pfleger *et al*, 2001). APC/C^{Cdh1} is involved in the degradation of Cyclin B1, CDC20, and Plk1, all of which are required for mitotic progression (Baker *et al*, 2007). Accordingly, MAD2L2-depleted cells show defective mitotic entry (Iwai *et al*, 2007). In other reports, MAD2L2-depleted cells exhibited a defective DNA damage response, suggesting that MAD2L2 is a functional homologue of yeast REV7 (Okada *et al*, 2005; Cheung *et al*, 2006). These data suggest that MAD2L2 has at least two functions, mitotic control and DNA damage response. However, its potential role in chromosome segregation has not been explored yet.

CAMP is a zinc-finger protein conserved in vertebrates and contains several characteristic repeat motifs. CAMP localizes to chromosomes and the spindle including kinetochores, and is phosphorylated during mitosis. Interestingly, it is involved in kinetochore–microtubule attachment in a way that maintains chromosome alignment on the metaphase plate. Our domain analyses identified a novel functional domain with the unique FPE repeat motifs responsible for the CAMP

*Corresponding author. Institute of Development, Aging and Cancer, Tohoku University, 4-1 Seiryo-machi, Aoba-ku, Sendai, Miyagi 980-8575, Japan. Tel./Fax: +81 22 717 8491;
E-mail: k.tanaka@idac.tohoku.ac.jp

Received: 8 May 2010; accepted: 19 October 2010; published online: 9 November 2010

function on proper chromosome segregation, which appears to be regulated by the mitotic phosphorylation.

Results

Identification of CAMP, a novel MAD2L2-interacting protein

To identify molecules that interact with MAD2L2 in human cells, we established HEK293 cells that stably expressed Flag-tagged MAD2L2, and performed immunoprecipitation (IP) of the cell extract with anti-Flag antibody. Bands that were detected in MAD2L2 IP, but not in control IP, were subjected to mass spectrometry, leading to the identification of C13orf8 (ZNF828; Supplementary Figure S1A). Based on its functions, the protein was designated CAMP. The interaction between Flag-MAD2L2 and CAMP was confirmed by IP-western analysis (Supplementary Figure S1B). Antibodies designed against CAMP recognized a polypeptide that migrated higher than its predicted molecular weight of 89 kDa. We also detected CAMP in Flag-MAD2L2 IPs prepared from both thymidine- and nocodazole-treated cells, showing that MAD2L2 interacts with CAMP both in the G1/S and M phases of the cell cycle (Supplementary Figure S1B). We further confirmed the interaction between MAD2L2 and CAMP by coimmunoprecipitation of the endogenous proteins (Figure 1A).

CAMP (C13orf8, ZNF828), an 812aa protein, contains two and three C2H2 zinc-finger domains in its N- and C-terminal regions, respectively (Supplementary Figure S1C). The protein is conserved among vertebrates, but has no apparent homologues in worms, flies, or yeast. CAMP contains several characteristic repeat motifs (Supplementary Figure S1C) that were designated as the SPE motif (consensus: PxxSPExxK), the WK motif (SPxxWKxxP), and the FPE motif (FPExxK). To examine the region of CAMP responsible for MAD2L2 interaction, CAMP was divided into four parts (Supplementary Figure S1D): the N-terminal region containing the zinc-finger domains and the six SPE motifs (N-ZNF; aa1–270), the middle region containing the SPE and WK motifs (WK: aa271–490), the adjacent middle region containing the FPE motifs (FPE: aa451–590), and the C-terminal region containing the zinc-finger domains (C-ZNF; aa591–812). We constructed a series of GST-fusion proteins, each containing a region of CAMP, and examined their interaction with MAD2L2 by far-western analysis (Supplementary Figure S1E). His-MAD2L2 bound to the WK region, indicating direct binding between CAMP and MAD2L2.

CAMP localizes to chromosomes and the spindle including kinetochores

The subcellular localization of CAMP was determined through immunofluorescence staining with an anti-CAMP antibody. During interphase, CAMP was detected in the nucleus (data not shown). In mitotic cells, CAMP was associated with chromosomes, and also localized to spindle fibres from prometaphase to anaphase (Figure 1B). Signal specificity was confirmed by disappearance of the signal after depletion of CAMP (data not shown). Consistent with the behavior of the endogenous protein, GFP-CAMP localized to both chromosomes and spindle fibres in metaphase cells (Figure 1C). To visualize the distribution of CAMP on chromosomes, we performed immunofluorescence staining of metaphase chromosome spreads. Dotty CAMP staining was distributed diffusely along chromosome arms (Supplementary Figure S1F). The CAMP signal was also visible on kinetochores stained with a human auto-antibody against kinetochore antigens (CREST serum; Supplementary Figure S1F).

Next, the region of CAMP responsible for chromosome and spindle localization was determined. HeLa cells were transfected with a series of GFP-fused CAMP-deletion mutants (Figure 1D). Neither the N-ZNF fragment (aa1–270) nor the WK fragment (aa271–490) of CAMP localized on chromosomes or the spindle fibres, while the C-ZNF fragment (aa591–812) localized both to chromosomes and the spindle (Figure 1C and D). Interestingly, the FPE fragment (aa451–590) did not localize to chromosomes, but did localize to the spindle fibres (Figure 1C and D). These results were confirmed by monitoring the localization of a CAMP-deletion mutant devoid of each region, as summarized in Figure 1D. CAMP mutants lacking the N-ZNF, SPE (aa143–290), WK (aa291–478), or FPE region localized both on chromosomes and the spindle, while the mutant lacking the C-ZNF region localized to the spindle, but not to the chromosomes (Figure 1D). Therefore, the FPE and C-ZNF region are independently involved in spindle localization, while the C-ZNF region is responsible for chromosome localization. The spindle localization of the FPE region included kinetochores at the end of spindle fibres, as the mutants containing the FPE region but lacking the C-ZNF region (GFP-CAMP-FPE, GFP-CAMP-ΔC-ZNF) were detected on kinetochores (Figure 1E and data not shown). Kinetochore localization of CAMP through the FPE region was clearly seen in prometaphase cells (Figure 1E) and nocodazole-treated cells (see Figure 7C), but also seen in metaphase cells at reduced levels (data not shown), suggesting that kinetochore–microtubule attachment reduces the level of CAMP on kinetochores.

CAMP is involved in chromosome alignment

To study the function of CAMP, we used siRNA to deplete CAMP in HeLa cells. Western blot analysis confirmed that CAMP protein levels decreased to $<10\%$ of normal 48 h after siRNA transfection (Figure 2A). MAD2L2 localized to the spindle as previously reported (Supplementary Figure S2A; Medendorp *et al*, 2009). We found that spindle localization of MAD2L2 was abolished by depletion of CAMP (Supplementary Figure S2A), while the expression of MAD2L2 was not altered (data not shown), suggesting that CAMP is required for the spindle localization of MAD2L2. We next assessed the role of CAMP on cell cycle progression. MAD2L2 has been reported to be involved in mitotic entry by inhibiting the activation of APC/C^{Cdh1} (Iwai *et al*, 2007). However, when the timing of mitotic entry in CAMP-depleted cells was measured, no apparent delay was observed (data not shown). Instead, mitotic indices were higher in CAMP-depleted cells than in mock-treated cells (Figure 2B), suggesting that depletion of CAMP resulted in defects in mitosis or mitotic exit. Observation of mitotic cells after depletion of CAMP revealed that a significant number of chromosomes were not aligned on the metaphase plate (Figure 2C). The percentage of cells with misaligned chromosomes after CAMP depletion was quantified by enriching the population of mitotic cells at metaphase with MG132 treatment. As shown in Figure 2E, chromosome misalignment was evident

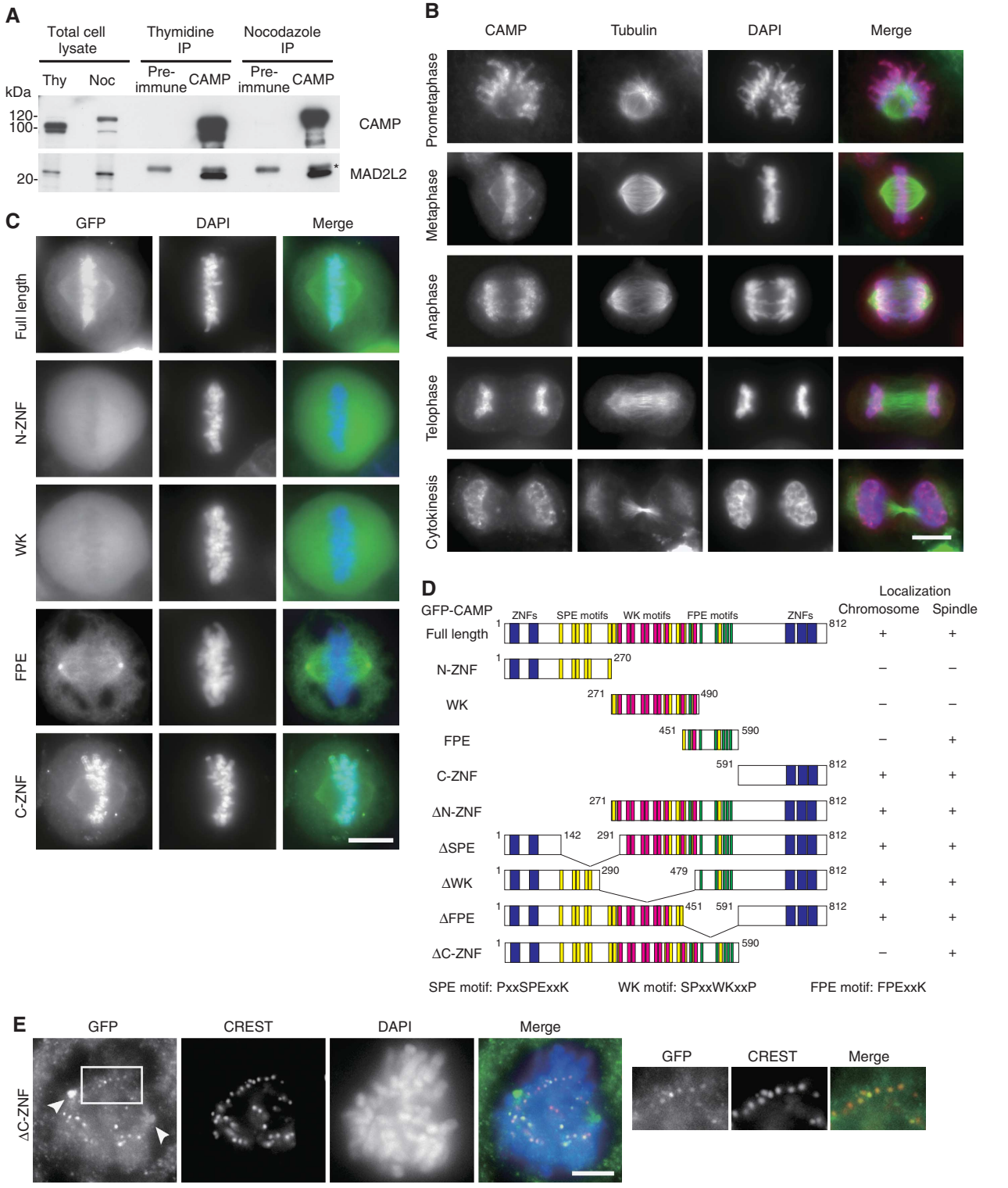

Figure 1 A MAD2L2-interacting protein, CAMP, localizes to chromosomes and the spindle including kinetochores. (**A**) Coprecipitation of endogenous CAMP with endogenous MAD2L2. Total cell lysates prepared from HeLa cells treated with thymidine or nocodazole were subjected to immunoprecipitation (IP) with anti-CAMP antibody. Lysates and IPs were separated by SDS–PAGE and probed by western blotting with anti-CAMP and anti-MAD2L2 antibodies, respectively. *IgG light chain. (**B**) Subcellular localization of CAMP during mitosis. HeLa cells were stained with anti-CAMP (red) and anti-tubulin (green) antibodies. DNA was stained with DAPI (blue). Scale bar = 10 μm. (**C**) Subcellular localization of CAMP fragments in metaphase. Localization of GFP-tagged full-length CAMP or each region of CAMP expressed in HeLa cells is shown (green). DNA was stained with DAPI (blue). Scale bar = 10 μm. (**D**) Summary of the subcellular localization of CAMP-deletion mutants. Localization of each mutant on chromosomes or the spindle is schematically shown, as indicated by either '+' or '−'. Sequences of the SPE, WK, and FPE motifs are shown. (**E**) Kinetochore localization of CAMP. Localization of GFP-CAMP-ΔC-ZNF expressed in HeLa cells is shown (green). Kinetochores were visualized with CREST serum (red) and DNA was stained with DAPI (blue). Arrowheads indicate spindle poles. Right panels are magnifications of the boxed areas. Scale bar = 5 μm.

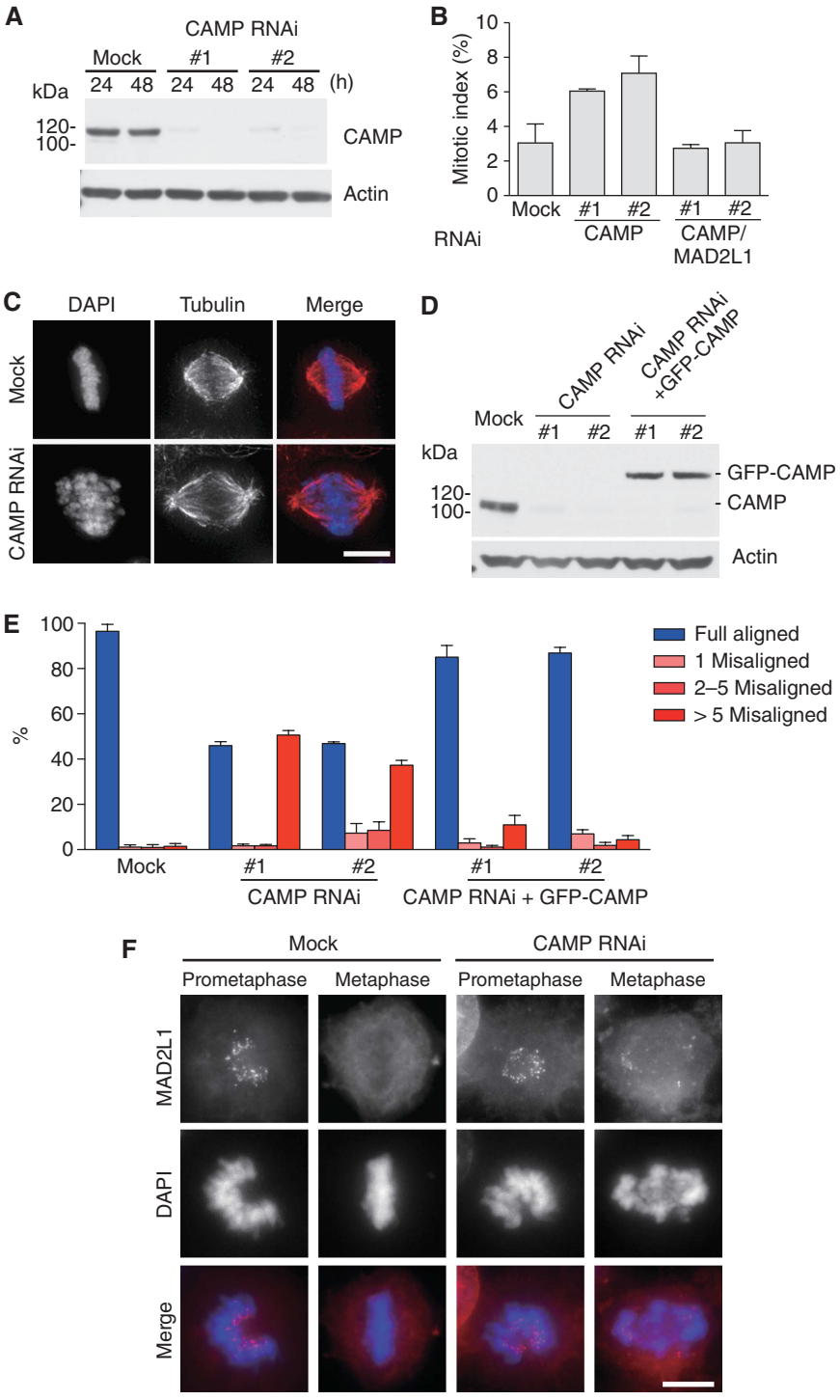

Figure 2 CAMP-depletion causes chromosome misalignment. (**A**) Depletion of CAMP with siRNAs. Total cell lysates prepared from HeLa cells treated with mock or CAMP siRNA for the indicated periods were separated by SDS–PAGE and probed by western blotting with anti-CAMP or anti-actin antibody. (**B**) Increased mitotic index in CAMP-depleted cells. The mitotic index for mock-, CAMP siRNA-, or CAMP/MAD2L1 siRNA-treated HeLa cells was measured 48 h after transfection. Error bars represent the s.d. (**C**) CAMP-depletion induced chromosome misalignment. HeLa cells treated with mock or CAMP siRNA for 48 h were stained with an anti-tubulin antibody (red). DNA was stained with DAPI (blue). Scale bar = 10 μm. (**D**) Expression of RNAi-resistant GFP-CAMP. Lysates were prepared from HeLa cells transfected with mock or CAMP siRNA with or without RNAi-resistant GFP-CAMP. The lysates were separated by SDS–PAGE and probed by western blotting with an anti-CAMP antibody. (**E**) Quantitative analysis of chromosome misalignment in CAMP-depleted cells. HeLa cells were transfected with RNAi-resistant GFP-CAMP constructs for 24 h, preceded by transfection with CAMP siRNA for 36 h. Cells were treated with MG132 (10 μM) for the final 2 h. The number of misaligned chromosomes per cell was scored. Error bars represent the s.d. (**F**) MAD2L1 localizes to kinetochores in CAMP-depleted cells. HeLa cells treated with mock or CAMP siRNA for 48 h were stained for MAD2L1 (red) and DNA (blue). Scale bar = 10 μm.

in nearly half of the CAMP-depleted cells. This phenotype was specific for CAMP depletion, as chromosome alignment was largely restored by the expression of RNAi-resistant GFP-CAMP (Figure 2D and E). Chromosome misalignment was also observed in U2OS cells depleted of CAMP (Supplementary Figure S2B). From these data, we concluded

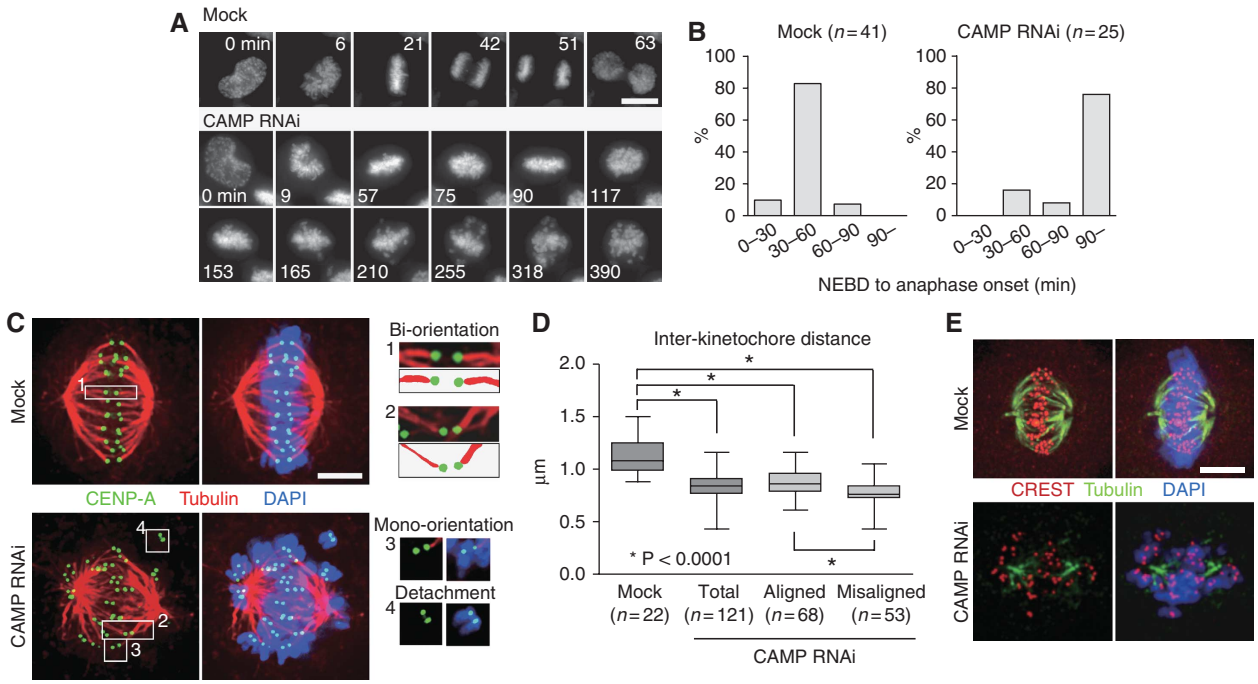

Figure 3 CAMP is required for proper kinetochore–microtubule attachment. (**A**) Live-cell imaging of HeLa cells expressing histone H2B-GFP, 48 h after mock- or CAMP-siRNA transfection. $T=0$ was defined as the time point at which chromosome condensation became evident (prophase). Scale bar = 10 μm. See also Supplementary Movies 1 and 2. (**B**) Prolonged mitosis in CAMP-depleted cells. HeLa cells were treated as in (**A**). The time from nuclear envelope breakdown (NEBD) to anaphase onset was measured in live-cell imaging and categorized. The percentages of cells in each category are shown in the graph. (**C**) Defective kinetochore–microtubule attachment in CAMP-depleted cells. HeLa cells expressing CENP-A-GFP (green) were treated with mock or CAMP siRNA for 48 h, and with MG132 for the final 2 h. Cells were stained for tubulin (red) and DNA (blue). Insets show individual kinetochore–microtubule attachments. Scale bar = 5 μm. (**D**) Quantitative analysis of inter-kinetochore distance in CAMP-depleted cells. HeLa cells expressing GFP-CENP-A were treated as in (**C**). The distance between CENP-A on sister kinetochores was measured. (**E**) Instability of kinetochore microtubules in CAMP-depleted cells. HeLa cells were treated as in (**C**), and then incubated on ice for 10 min before fixation. Cells were stained for kinetochores (CREST, red), tubulin (green) and DNA (blue). Scale bar = 5 μm.

that CAMP is crucial for proper chromosome alignment on the metaphase plate.

CAMP-depleted cells with misaligned chromosomes remained in mitosis (see Figure 3B) and MAD2L1 was detected on kinetochores of misaligned chromosomes (Figure 2F), suggesting that the SAC was not satisfied. Indeed, the increase in mitotic indices induced by CAMP depletion could be overcome by codepletion of MAD2L1 (Figure 2B). These data suggest that normal levels of CAMP are not necessary for the SAC.

Defective kinetochore–microtubule attachment in CAMP-depleted cells

To examine the mechanism of chromosome misalignment in CAMP-depleted cells, we observed HeLa cells expressing histone H2B-GFP with live-cell imaging, with or without CAMP depletion. As shown in Figure 3A, in the majority of mock-treated cells, chromosomes were properly aligned and quickly segregated within an hour of nuclear envelope breakdown (Figure 3B; Supplementary Movie 1). In contrast, in CAMP-depleted cells, the alignment of chromosomes was delayed (Figure 3A, 57 min) and, subsequently, chromosomes began to leave the metaphase plate instead of being segregated (Figure 3A, 153 min), resulting in massive chromosome misalignment (Supplementary Movie 2). During mitotic arrest, rotation of the spindle axis was observed (Figure 3A, 57–153 min), as well as multipolar spindle formation (Supplementary Figure S3A). The majority of CAMP-depleted cells were arrested in mitosis (Figure 3B), and eventually died with multiple misaligned chromosomes. In summary, CAMP-depleted cells exhibited delayed chromosome alignment and were unable to maintain that alignment while arrested during mitosis.

To address the underlying cause of the chromosome misalignment in CAMP-depleted cells, cells were treated with MG132 and examined by immunofluorescence staining. In mock-treated cells, each pair of kinetochores on sister chromatids were aligned on the metaphase plate and were pulled towards opposite spindle poles with robust K-fibres (Figure 3C, inset 1), whereas in CAMP-depleted cells, many chromosomes were not aligned on the metaphase plate (Figure 3C). However, kinetochores on misaligned chromosomes were still paired, indicating that precocious separation of sister chromatids had not occurred. These misaligned sister chromatid pairs often attached to only one kinetochore, or did not attach at all to the microtubules (Figure 3C, insets 3 and 4). Even when both sister kinetochore pairs were attached to microtubules, K-fibre thickness was irregular (Figure 3C, inset 2), suggesting that tension was not properly exerted between the sister kinetochores. Consistent with this idea, inter-kinetochore distance in CAMP-depleted cells was shorter than in mock-treated cells, for both misaligned and aligned chromosomes (Figure 3D). To examine the stability of the kinetochore–microtubule attachment, MG132-treated cells were exposed to low temperatures, which induced the disassembly of unstable microtubules. In mock-treated cells,

thick K-fibres were clearly attached to each kinetochore (Figure 3E), whereas in CAMP-depleted cells, few cold-stable K-fibres were observed (Figure 3E). These results indicate that defective kinetochore–microtubule attachment caused mitotic delay and subsequent collapse of metaphase plate in CAMP-depleted cells.

K-fibres cannot resist tension in CAMP-depleted cells

To dissect further the relationship between failure to maintain chromosome alignment and defective kinetochore–microtubule attachment in CAMP-depleted cells, we monitored kinetochore–microtubule attachment by live-cell imaging of HeLa cells expressing GFP-CENP-A and GFP-α-tubulin. In mock-treated cells, kinetochores were quickly captured by microtubules before their transport to the metaphase plate. Thick K-fibres were established in these cells during metaphase (Supplementary Movie 3). In CAMP-depleted cells, even when the majority of chromosomes were found on the metaphase plate, kinetochore-attached microtubules never progressed into thick K-fibres (Figure 4A; Supplementary Movie 4). Instead of inducing anaphase, kinetochore pairs were gradually displaced from the metaphase plate during prolonged mitotic arrest. A careful inspection of a kinetochore pair movement in CAMP-depleted cells revealed that the kinetochore pair first moved close to the metaphase plate, attached to microtubules from opposite spindle poles establishing amphitelic attachment (Figure 4A, 0 min). The kinetochore pair was then pulled to one of the spindle poles, while it remained attached to microtubules on both kinetochores (Figure 4A, 9–11 min). At 13 min, attachment to microtubules at the trailing kinetochore was no longer visible, most likely reflecting kinetochore detachment from the microtubules. After that, the kinetochore pair was quickly pulled to a spindle pole by microtubules attached to the leading kinetochore (Figure 4A, 14–21 min). These observations suggest that kinetochore–microtubule attachment was not maintained properly during bi-orientation in CAMP-depleted cells, which eventually caused chromosome misalignment.

The above phenotype can be attributable to either defective K-fibre maturation or unstable kinetochore–microtubule attachment, or both. We first monitored the process of K-fibre maturation in the absence of tension in cells treated with monastrol, a kinesin-5 (Eg5) inhibitor. K-fibres on monopolar spindles in CAMP-depleted cells were not distinguishable from those in mock-treated cells (Figure 4B), suggesting that K-fibre maturation *per se* in these cells was proficient. Consistent to this, γ-tubulin localized to the spindle in CAMP-depleted cells (Supplementary Figure S3B), which is required for bundling microtubules via the augmin complex/HAUS (Lawo *et al*, 2009; Uehara *et al*, 2009). In addition, nucleation of microtubules at kinetochores, which also contributes to K-fibre formation (Khodjakov *et al*, 2003; Maiato *et al*, 2004), was observed in CAMP-depleted cells released from nocodazole treatment, similar to mock-treated cells (data not shown; Tulu *et al*, 2006). The K-fibre stability of the monopolar spindles was further assessed by exposing monastrol-treated cells to low temperatures. Remarkably, the microtubules that remained in CAMP-depleted cells were shorter and thinner than those in mock-treated cells (Figure 4C), showing that K-fibres were unstable before the application of tension. This could be either due to defective kinetochore–microtubule attachment, or destabilization of kinetochore–microtubule attachments secondary to abnormal microtubule dynamics. From these data, it can be concluded that kinetochore–microtubule attachments in CAMP-depleted cells are not robust enough to resist the tension exerted upon establishment of bi-orientation.

The FPE region is required for proper chromosome alignment by CAMP

To determine the region of CAMP responsible for controlling kinetochore–microtubule attachment, we examined chromosome alignment in CAMP-depleted HeLa cells expressing a series of RNAi-resistant GFP-CAMP-deletion mutants in the presence of MG132. Comparable expression of each construct was confirmed by western blotting (Supplementary Figure S4A). Cells that expressed GFP alone showed massive chromosome misalignment after CAMP depletion, while chromosome misalignment was largely rescued in cells that expressed GFP-tagged full-length CAMP (Figure 5A). We next determined which region was required to restore the phenotype under these conditions. Cells expressing GFP-CAMP devoid of the N-terminal region, the SPE region, the WK region, or the C-terminal region showed a level of chromosome misalignment similar to that of cells expressing full-length CAMP, indicating that these regions are dispensable for chromosome alignment (Figure 5A). However, GFP-CAMP devoid of the FPE region failed to rescue chromosome misalignment, suggesting that the FPE region mediates chromosome alignment (Figure 5A). Similar results were obtained with Flag-tagged CAMP constructs (Supplementary Figure S4B). Complementary to these results, we then tested the effect of GFP-CAMP fragments on chromosome alignment when expressed in CAMP-depleted cells. As expected, expression of the FPE region significantly rescued chromosome misalignment, whereas expression of the N-terminal region (N-ZNF), the WK region, or the C-terminal region (C-ZNF) did not (Figure 5B). Comparable expression of each fragment was confirmed by western blotting (Supplementary Figure S4C). These data demonstrate that the FPE region is required and sufficient for rescuing chromosome misalignment in CAMP-depleted cells, and confirmed the role of the FPE region in kinetochore–microtubule attachment. Considering the localization of the FPE region to the spindle and kinetochores (Figures 1C–E and 7C), it is plausible that CAMP molecules localized to the spindle and kinetochores are primarily involved in the regulation of kinetochore–microtubule attachment.

Mitotic phosphorylation of CAMP is essential for chromosome alignment

Although expression of CAMP did not significantly change during the cell cycle (data not shown), CAMP from nocodazole-treated cells migrated more slowly during SDS–PAGE compared with CAMP from thymidine-treated cells (Figure 1A; Supplementary Figure S1B), suggesting post-translational modifications during mitosis. Treatment of lysates from cells arrested in mitosis with λ-phosphatase resulted in faster migration of CAMP, indicating that the observed retardation in electrophoretic mobility was dependent on phosphorylation (Figure 6A). Notably, λ-phosphatase treatment also resulted in a slightly faster migration of CAMP

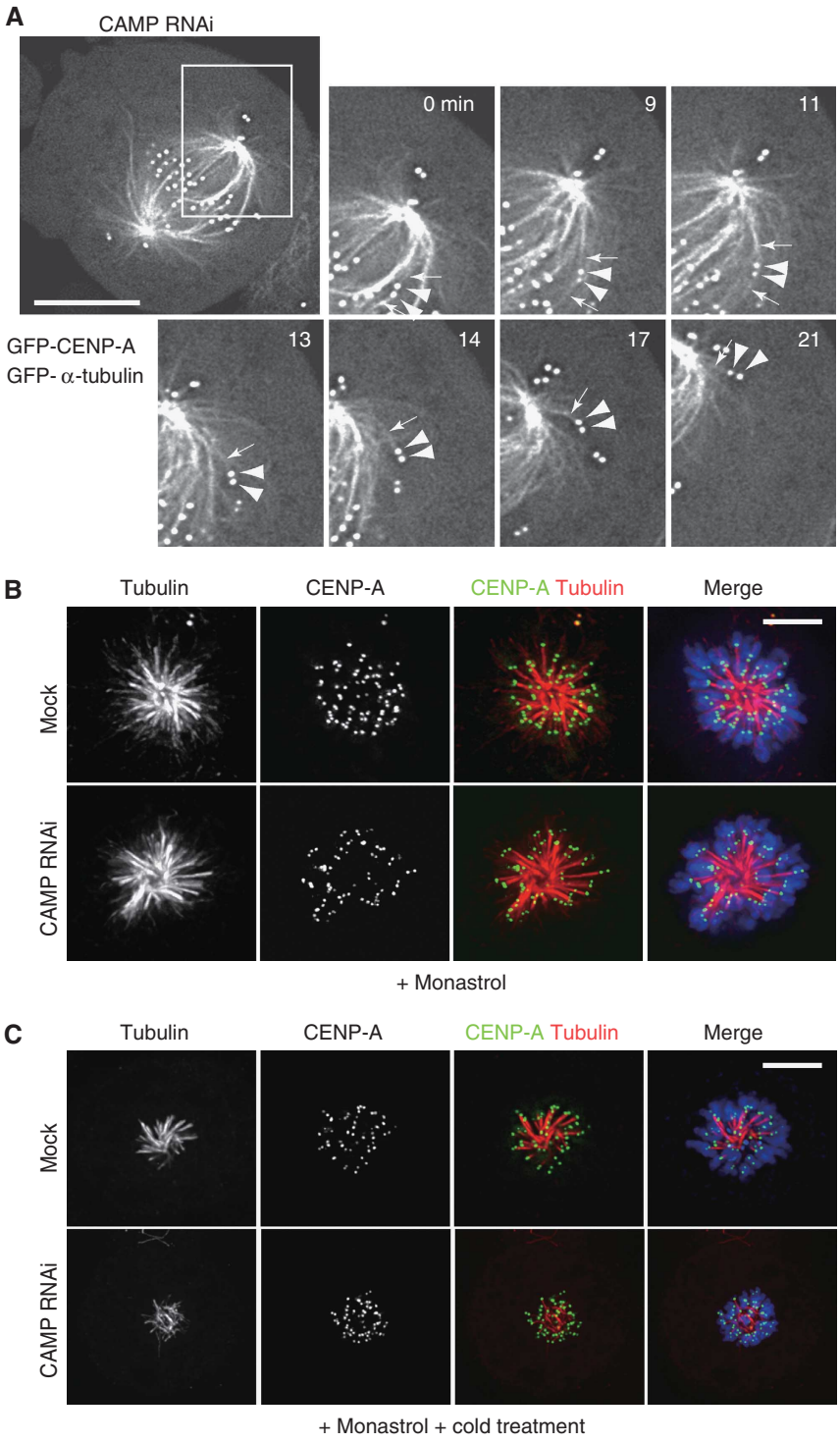

Figure 4 K-fibres cannot resist tension in CAMP-depleted cells. (**A**) Disruption of kinetochore–microtubule attachment in CAMP-depleted cells. HeLa cells expressing GFP-CENP-A and GFP-α-tubulin were treated with CAMP siRNA for 48 h before live-cell imaging. $T = 0$ was set arbitrarily for the first panel. Arrowheads indicate kinetochores on a sister chromatid pair. Arrows indicate microtubules attached to these kinetochores. Scale bar = 10 μm. See also Supplementary Movie 4. (**B**) K-fibres on a monopolar spindle in CAMP-depleted cells. HeLa cells expressing GFP-CENP-A (green) were treated with mock or CAMP siRNA for 48 h, and with monastrol (100 μM) for the final 2 h before fixation. Cells were stained for tubulin (red) and DNA (blue). Scale bar = 5 μm. (**C**) Instability of K-fibres on monopolar spindles in CAMP-depleted cells. HeLa cells expressing GFP-CENP-A (green) were treated with mock or CAMP siRNA for 48 h and with monastrol (100 μM) for the final 2 h, and then incubated on ice for 10 min before fixation. Cells were stained for tubulin (red) and DNA (blue). Scale bar = 5 μm.

from thymidine-treated cells, suggesting that phosphorylation occurs also in interphase (Figure 6A).

CAMP has numerous characteristic SPE/D sequences (22 in total; Supplementary Figure S5A), many of which are clustered in regions designated as SPE motifs (Supplementary Figure S1C). To examine whether serine residues in the SPE/D sequences are phosphorylated during mitosis, a GFP-CAMP mutant was constructed in which all of the 22 serines in the

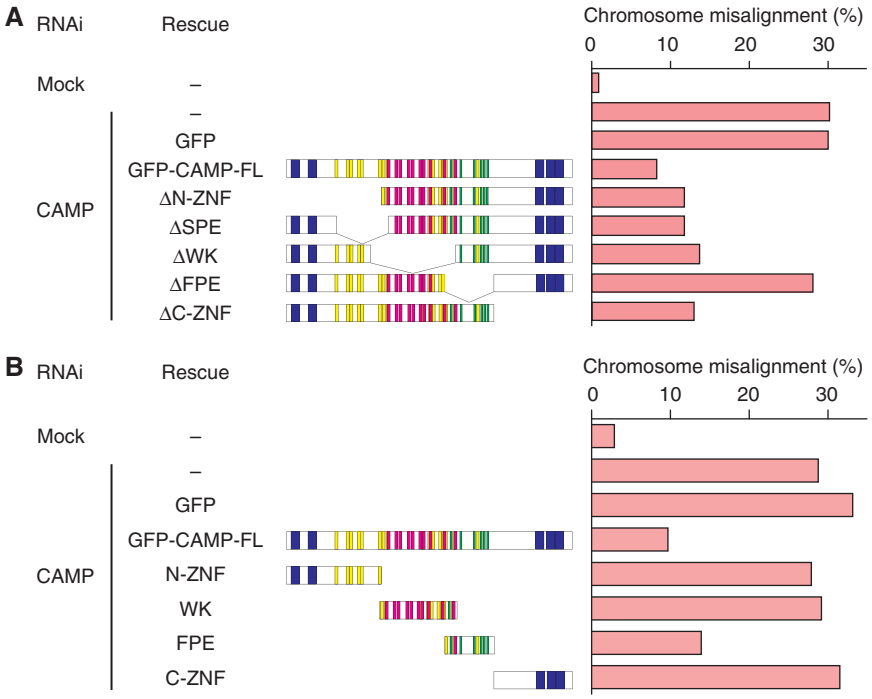

Figure 5 The FPE region of CAMP is responsible for chromosome alignment. (**A**, **B**) HeLa cells were transfected with RNAi-resistant GFP-CAMP constructs for 24 h, preceded by transfection with CAMP siRNA for 36 h. Cells were treated with MG132 for the final 2 h. The structures of these constructs are the same as shown in Figure 1D. A CAMP-deletion construct lacking each domain was used in (**A**), while a CAMP fragment containing each domain was used in (**B**). The percentage of cells with misaligned chromosomes is shown for cells expressing each construct. Experiments were repeated three times and representative data are shown. Oligo 1 was used for RNAi; similar results were obtained for oligo 2 (data not shown).

SPE/D sequences were mutated to alanines (GFP-CAMP-22A). In cells treated with nocodazole, GFP-CAMP-22A migrated faster than GFP-CAMP, mostly abolishing the band shift (Figure 6B). This suggests that serines in the SPE/D sequences were phosphorylated in mitosis. We examined the involvement of CDK1, a major proline-directed serine/threonine kinase in mitosis, in the phosphorylation of CAMP. In the presence of RO-3306, a CDK1 inhibitor, the band shift of CAMP in nocodazole-treated cells partially decreased, suggesting that mitotic phosphorylation of CAMP is dependent on CDK1 (Figure 6C). This result also suggests that kinases other than CDK1 phosphorylate CAMP as well. To identify other kinases involved in CAMP phosphorylation, we further examined whether the migration velocity of CAMP in nocodazole-treated cells was affected by suppression of a series of mitotic kinases, either by the addition of specific inhibitors (Aurora B, Plk1, MAPK) or depletion of kinases with siRNAs (MPS1, BUB1, BUBR1), but no change in the mobility of CAMP was observed in response to any of these treatments (data not shown).

To address whether the phosphorylation state of CAMP during mitosis affects its role on chromosome alignment, we examined the alignment of chromosomes in cells expressing non-phosphorylatable CAMP mutants under the metaphase-arrested condition (Supplementary Figure S5B). Cells in which endogenous CAMP was replaced with GFP-CAMP-22A exhibited a significant number of misaligned chromosomes, while cells in which CAMP was replaced with GFP-tagged wild-type CAMP did not (Figure 6D). Similar results were obtained when Flag-tagged CAMP constructs were expressed instead of GFP-tagged constructs (data not shown). These data suggest that the mitotic phosphorylation of CAMP is required for the function of CAMP to maintain chromosome alignment.

As the domain analysis above suggested that the FPE region, which by itself localizes to the spindle and kinetochores, is required to control chromosome alignment (Figure 5A and B), it was possible that mitotic phosphorylation of CAMP regulated its spindle/kinetochore localization. However, as shown in Supplementary Figure S5C, GFP-CAMP-22A was detected on the chromosomes and the spindle in a pattern similar to wild-type CAMP. This was also the case for GFP-CAMP-ΔC-ZNF-22A and GFP-CAMP-FPE-3A, which are non-phosphorylatable CAMP mutants that lack C-ZNF, another region capable of associating with the spindle (Supplementary Figure S5C). These data show that the mitotic phosphorylation does not affect the spindle/kinetochore localization of CAMP via the FPE region. Surprisingly, however, unlike in cells expressing GFP-CAMP-22A, chromosome alignment was largely rescued in cells expressing non-phosphorylatable mutants of CAMP that lack the C-terminal region (GFP-CAMP-ΔC-ZNF-22A and GFP-CAMP-FPE-3A) in place of endogenous CAMP (Figure 6D). This suggests that the C-terminal region negatively regulates the function of the FPE region, which requires mitotic phosphorylation. In line with this idea, a non-phosphorylatable CAMP mutant comprising the FPE region and the C-terminal region (GFP-CAMP-FPE-C-ZNF-3A) was unable to rescue chromosome misalignment induced by CAMP depletion, when the corresponding phosphorylatable mutant could (Figure 6D). These results imply that phosphorylation in the FPE region is responsible for preventing the inhibitory effect of the C-terminal region.

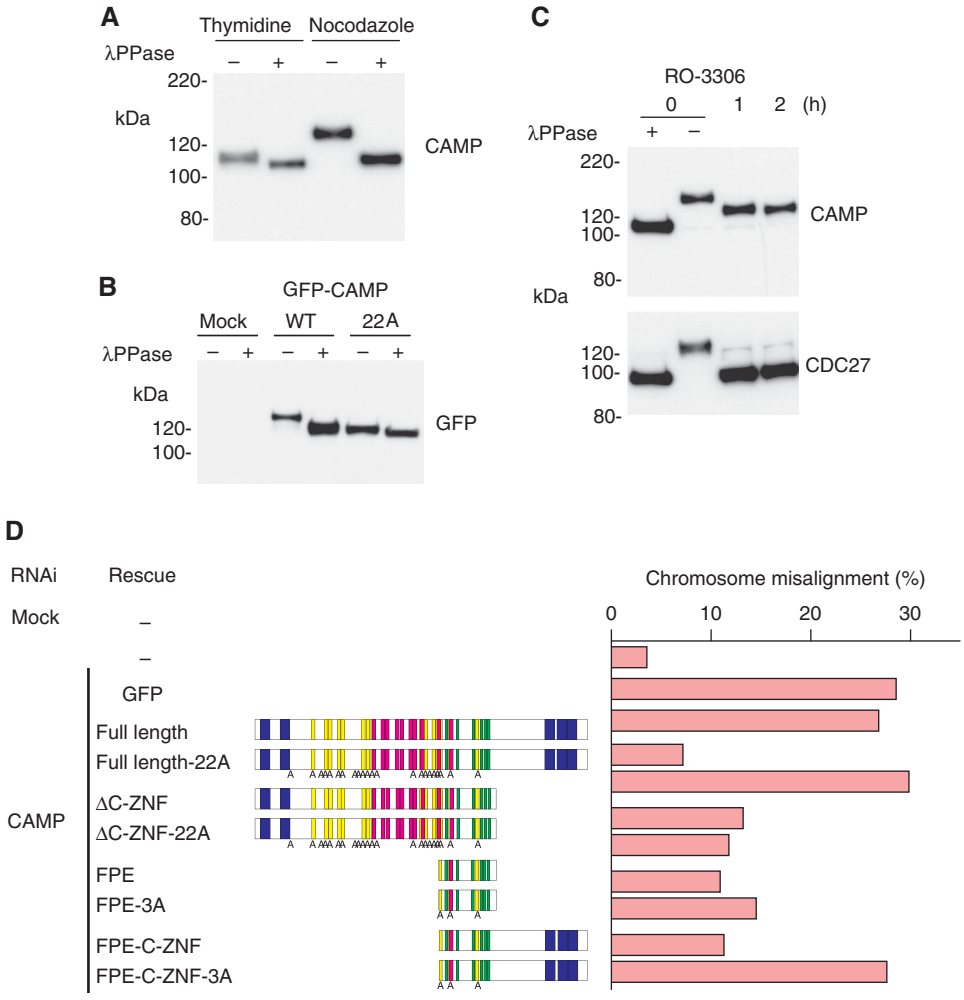

Figure 6 Phosphorylation of CAMP during mitosis is essential for chromosome alignment. (**A**) CAMP is phosphorylated during mitosis. Total cell lysates prepared from HeLa cells treated with thymidine or nocodazole were incubated in the absence (−) or presence (+) of λ-phosphatase for 30 min at 30°C. Equal amounts of cell lysates were separated by SDS–PAGE and probed by western blotting with an anti-CAMP antibody. (**B**) CAMP is phosphorylated at serine residues in the SPE/D sequences. Lysates were prepared from nocodazole-treated HeLa cells expressing GFP-tagged CAMP with (GFP-CAMP-22A) or without mutations in the serine residues in the SPE/D sequences. Equal amounts of cell lysates were separated by SDS–PAGE and probed by western blotting with an anti-GFP antibody. (**C**) CDK1-dependent phosphorylation of CAMP. HeLa cells were treated with nocodazole for 12 h after thymidine treatment, and with RO-3306 (CDK1 inhibitor; 10 μM) for the time indicated. Total cell lysate at $T=0$ was incubated in the presence (+) or absence (−) of λ-phosphatase for 30 min at 30°C. Equal amounts of cell lysates were separated by SDS–PAGE and probed by western blotting with an anti-CAMP or anti-CDC27 antibody. (**D**) Mitotic phosphorylation of CAMP is essential for chromosome alignment. HeLa cells were transfected with RNAi-resistant GFP-CAMP constructs for 24 h, preceded by transfection with CAMP siRNA for 36 h. Cells were treated with MG132 for the final 2 h. The structures of these constructs are schematically represented; each serine residue that was replaced with alanine is indicated by 'A'. The percentage of cells with misaligned chromosomes is shown for cells expressing each construct. Experiments were repeated three times and representative data are presented. Oligo 1 was used for RNAi; similar results were obtained for oligo 2 (data not shown).

Decreased kinetochore localization of CENP-E and CENP-F correlates with chromosome misalignment in CAMP-depleted cells

To investigate the role of CAMP in controlling kinetochore–microtubule attachments, we asked if the localization of kinetochore/centromere proteins involved in mediating kinetochore–microtubule attachment (Musacchio and Salmon, 2007) was affected in CAMP-depleted cells. No obvious change in the kinetochore/centromere localization of CENP-C, HEC1, Aurora B, Blinkin (KNL1), RanGAP1, RanBP2, Sgo1, or Ska1 was detected in CAMP-depleted cells compared to mock-treated cells (Supplementary Figure S6A and B). Phosphorylation levels of histone H3 on serine 10 were not affected in CAMP-depleted cells, implying that Aurora B kinase activity was intact (Supplementary Figure S7B). Spindle localization of plus-end tracking proteins (+TIPs) EB1, CLIP-170, and ch-TOG, which regulate microtubule dynamics and chromosome segregation (Cassimeris and Morabito, 2004; Green *et al*, 2005; Draviam *et al*, 2006; Tanenbaum *et al*, 2006; De Luca *et al*, 2008), was not affected by CAMP depletion (Supplementary Figure S7A). The chromosome/spindle localization of Kid, a motor protein that facilitates chromosome alignment (Tokai-Nishizumi *et al*, 2005), was not altered in CAMP-depleted cells (Supplementary Figure S7C), either. We also observed the unperturbed centromeric localization of HP1α, depletion of which leads to chromosome misalignment (Kiyomitsu *et al*, 2010), after CAMP depletion (Supplementary Figure S7D).

BUB1, BUBR1, and CENP-E are unambiguously found on unattached kinetochores, which are known to decrease upon kinetochore attachment to microtubules (Hoffman *et al*, 2001; Howell *et al*, 2004). However, in CAMP-depleted cells, BUB1 and BUBR1 localization on kinetochores was increased, even on properly aligned chromosomes, which likely reflects defective kinetochore–microtubule attachment (Supplementary Figure S6C). Conversely, we noticed that CENP-E was decreased on kinetochores in CAMP-depleted cells as well as another component of outer kinetochore, CENP-F (Figure 7A and B). It was not only evident when we compare kinetochore levels of these proteins between metaphase chromosomes in mock-treated cells and seemingly 'aligned' chromosomes in CAMP-depleted cells, but also when we compare prometaphase chromosomes (before or during kinetochore–microtubule attachment) in mock-treated cells with misaligned chromosomes in CAMP-depleted cells (Figure 7A and B). Western blotting showed that cellular levels of CENP-E and CENP-F were unchanged after CAMP depletion (see Supplementary Figure S8A). Consistently with the notion that CAMP affects the localization of CENP-E and CENP-F on kinetochores, we observed colocalization of the FPE region of CAMP with CENP-E and CENP-F on kinetochores in nocodazole-treated cells, where CENP-E and CENP-F typically showed crescent shape (Figure 7C). Similar to CAMP-depleted cells, delayed chromosome congression and unstable kinetochore–microtubule attachments were seen in live-cell imaging of CENP-E or CENP-F-depleted cells (data not shown), as previously reported (Schaar *et al*, 1997; McEwen *et al*, 2001; Holt *et al*, 2005; Laoukili *et al*, 2005; Yang *et al*, 2005; Feng *et al*, 2006). These data therefore raises an intriguing possibility that decreased kinetochore localization of CENP-E and CENP-F accounts for defective kinetochore–microtubule attachments after CAMP depletion.

To investigate whether the decreased kinetochore localization of CENP-E and CENP-F contributes to the chromosome misalignment phenotype in CAMP-depleted cells, we compared the rates of chromosome misalignment between cells depleted of CAMP, CENP-E, and CENP-F (Supplementary Figure S8A). CAMP- and CENP-E-depleted cells showed comparable misalignment rates, while CENP-F-depleted cells exhibited chromosome misalignment less frequently (Figure 7D). Importantly, when CAMP was depleted together with CENP-E or CENP-F, additive effect was not seen (Figure 7D). This was also the case when CAMP, CENP-E, and CENP-F were depleted simultaneously (Figure 7D). These data suggest that these proteins are working in the same pathway.

To further investigate the significance of CAMP in kinetochore localization of CENP-E and CENP-F, we tested how might kinetochore localization of CENP-E and CENP-F relate with the chromosome misalignment phenotype in cells expressing a series of phosphorylation mutants of CAMP. As shown in Figure 7E and Supplementary Figure S9, kinetochore levels of CENP-E/CENP-F was recovered when chromosome misalignment was rescued by GFP-tagged wild-type CAMP both on prometaphase and metaphase chromosomes, but not by GFP-CAMP-22A (non-phosphorylatable mutant). When we compared the kinetochore levels of CENP-E/CENP-F on 'aligned' chromosomes between cells expressing phosphorylation mutants of CAMP used in Figure 6D, they were clearly recovered in cells with CAMP mutants that rescue chromosome misalignment, while they remained decreased in cells expressing mutants that were unable to rescue chromosome misalignment (GFP-CAMP-FL-22A, GFP-CAMP-FPE-C-ZNF-3A; Figure 7F; Supplementary Figure S9). These data reveal a strong correlation between kinetochore localization of CENP-E/CENP-F and the function of CAMP to regulate kinetochore–microtubule attachment, supporting the notion that CENP-E and CENP-F are effectors of CAMP for the regulation of kinetochore–microtubule attachment.

Discussion

In this paper, we report the identification of a novel protein CAMP, a phosphoprotein containing unique repeat motifs, which appears to be involved in kinetochore–microtubule attachment. In addition to the canonical C2H2 zinc-finger domains, CAMP contains several characteristic repeat motifs (Supplementary Figure S1C; Figure 8). Among them, the SPE motifs contain serine residues that are phosphorylated during mitosis. The WK motifs, which partially overlap with the SPE motifs, mediate the interaction between CAMP and MAD2L2 (Supplementary Figure S1E). Spindle localization of MAD2L2 was abrogated by CAMP depletion (Supplementary Figure S2A), although the role of MAD2L2 on the spindle has not been clarified yet (Medendorp *et al*, 2009). We did not observe a delay in mitotic entry in CAMP-depleted cells (data not shown) as was reported for MAD2L2-depleted cells (Iwai *et al*, 2007). We also did not observe chromosome misalignment in MAD2L2-depleted cells (Supplementary Figure S2A), and the WK region was found to be dispensable for chromosome alignment (Figure 5A and B). Thus, the functional relationship between CAMP and MAD2L2 awaits further investigation. The region containing the FPE motifs is involved in spindle/kinetochore localization, but not in chromosome localization (Figures 1C–E and 7C), and is essential for chromosome alignment (Figure 5A and B). The C-terminal region containing the zinc-finger domains is involved in the localization of CAMP to both chromosomes and the spindle (Figure 1C and D), and has an inhibitory effect on chromosome alignment (Figure 6D). Concerning the localization of CAMP throughout chromosome length, we examined the localizations of the chromokinesin Kid, HP1α, condensin I and II, all of which are found on chromosomes, as well as the phosphorylation status of serine 10 or threonine 3 of histone H3 (Dai *et al*, 2005; Supplementary Figure S7B–E). We did not observe any difference in CAMP-depleted cells compared with mock-treated cells, leaving the function of chromosome-localized CAMP an unanswered question. CAMP is a unique protein, which does not form an ordered structure other than zinc-finger domains, as predicted by the PrDOS server (http://prdos.hgc.jp/cgi-bin/top.cgi; Ishida and Kinoshita, 2007). Disordered regions are frequently involved in interaction with other proteins and often contain phosphorylation sites (Iakoucheva *et al*, 2004; Dyson and Wright, 2005). CAMP may have multiple functions mediated by the disordered regions containing characteristic repeat motifs. Investigation of the structures and functions of these motifs and search for similar motifs in other proteins are important future directions.

Our data suggest that kinetochore–microtubule attachment in CAMP-depleted cells was too weak to resist tension applied between sister kinetochores. How does CAMP regulate kinetochore–microtubule attachment? The FPE region, which can localize spindle/kinetochores (Figures 1C–E and 7C), was

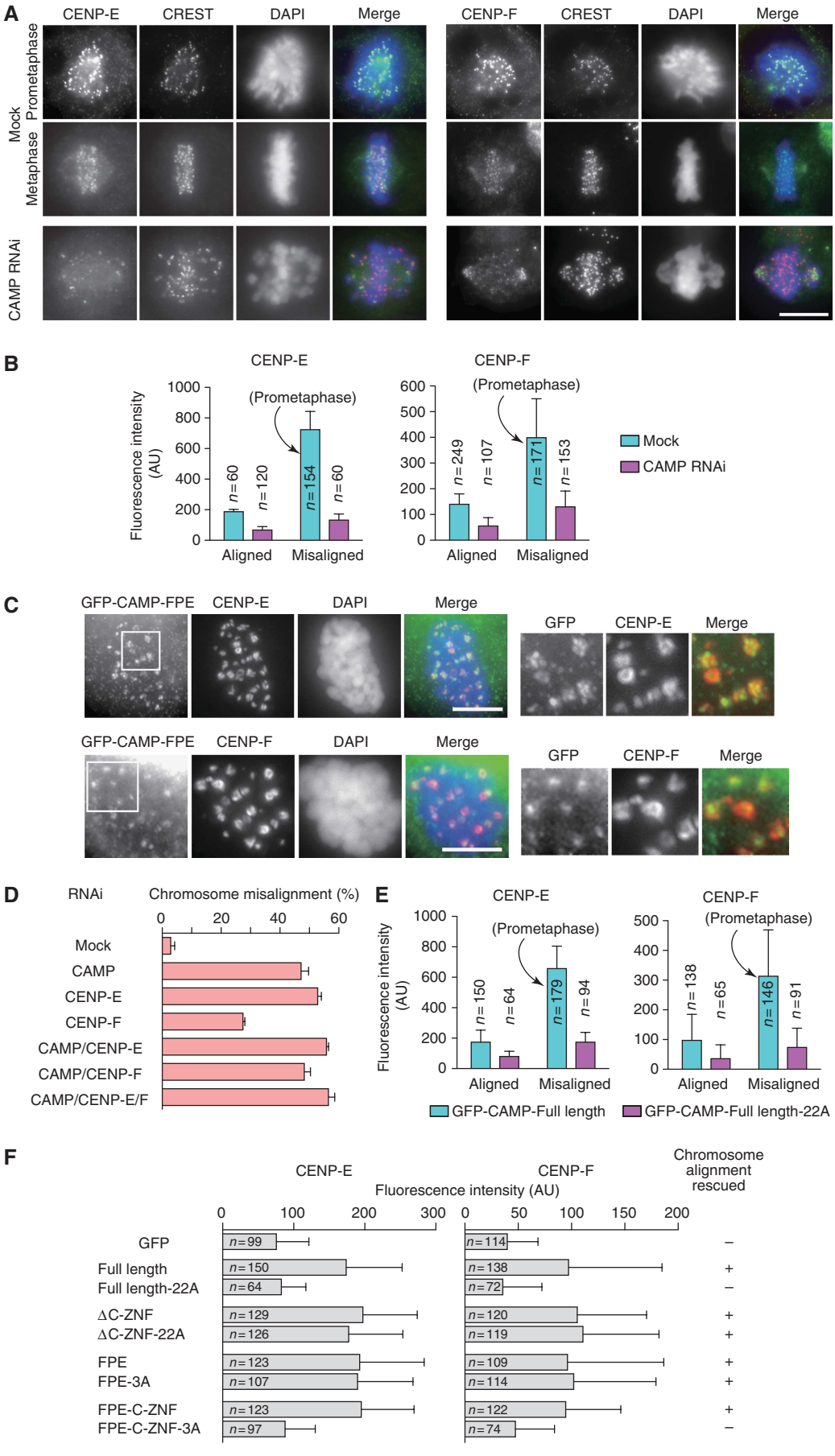

found to be essential for the function (Figure 5A and B). As CAMP did not bind to microtubules in our *in vitro* assay (SC, KM, and KT unpublished observations), we consider it unlikely that CAMP is involved directly in kinetochore–microtubule interaction at kinetochores. Therefore, one plausible possibility is that CAMP affects the localization/function of other molecules involved in kinetochore–microtubule attachment on spindle/kinetochores. We found that CENP-E and CENP-F decreased on kinetochores in CAMP-depleted cells (Figure 7A and B). CENP-E and CENP-F reside at the kinetochore–microtubule interface and are involved in stabilizing the binding of microtubules to kinetochores (Yao *et al*, 2000; McEwen *et al*, 2001; Putkey *et al*, 2002; Bomont *et al*, 2005; Feng *et al*, 2006; Vergnolle and Taylor, 2007). CENP-E and CENP-F are closely related proteins, as they are known to interact each other and their kinetochore localization is interdependent (Chan *et al*, 1998; Johnson *et al*, 2004). Moreover, both are farnesylated, which is crucial for their mitotic functions (Ashar *et al*, 2000; Hussein and Taylor, 2002; Schafer-Hales *et al*, 2007). Colocalization of CAMP with CENP-E/CENP-F on kinetochores (Figure 7C) and the strong correlation between CAMP functionality and CENP-E/CENP-F levels on kinetochores (Figures 6D and 7F; Supplementary Figure S9) supports the notion that CAMP regulates targeting CENP-E/CENP-F to kinetochores. Kinetochore localization of CENP-E/CENP-F is regulated directly by interaction with other kinetochore components (Chan *et al*, 1998; Johnson *et al*, 2004; Liu *et al*, 2007), or indirectly by posttranslational modifications (Schafer-Hales *et al*, 2007; Zhang *et al*, 2008). As we found no evidence for physical interaction between CAMP and CENP-E/CENP-F (unpublished data), CAMP may regulate localization of CENP-E/CENP-F indirectly through one of these mechanisms. Lack of additive effects on chromosome misalignment when CAMP and CENP-E/CENP-F were simultaneously depleted (Figure 7D) suggests that CENP-E and CENP-F are downstream of CAMP in mitotic function. When we quantified the number of misaligned chromosomes per cell, however, more chromosomes were misaligned in CAMP-depleted cells compared to CENP-E/CENP-F-depleted cells (Supplementary Figure S8B and C), suggesting that targeting CENP-E/CENP-F to kinetochores is not the only mechanism for chromosome alignment by CAMP.

Another possibility is that CAMP may function as a (indirect) microtubule-associated protein to regulate microtubule dynamics necessary for proper chromosome

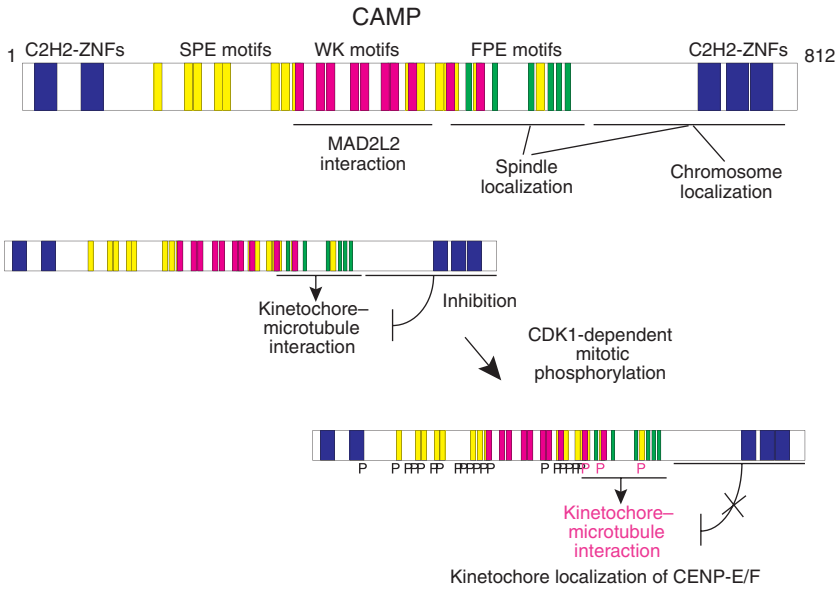

Figure 8 Schematic diagram of CAMP structure with regard to the functions revealed in this study. Each serine residue phosphorylated during mitosis is indicated by 'P'. See text for details.

Figure 7 Decreased kinetochore localization of CENP-E and CENP-F correlates with chromosome misalignment by CAMP mutants. (**A**) Decreased CENP-E and CENP-F on kinetochores in CAMP-depleted cells. HeLa cells were treated with mock or CAMP siRNA for 48 h and with MG132 for the final 2 h. Cells were stained for CENP-E or CENP-F (green), CREST (red), and DNA (blue). Scale bar = 10 μm. (**B**) Quantification of fluorescence intensity (arbitrary unit; AU) of the CENP-E or CENP-F signal at kinetochores on aligned or misaligned chromosomes. Misaligned chromosomes in mock-transfected cells were selected in prometaphase cells. Error bars represent the s.d. (**C**) Colocalization of CAMP with CENP-E/CENP-F on kinetochores in nocodazole-treated cells. Localization of GFP-CAMP-FPE expressed in HeLa cells treated with nocodazole (2 μM) is shown (green), together with CENP-E/CENP-F (red) and DNA (blue). Right panels are magnifications of the boxed areas. Scale bars = 5 μm. (**D**) Quantitative analysis of chromosome misalignment in cells depleted of CAMP/CENP-E/CENP-F. HeLa cells were transfected with the indicated siRNAs for 48 h, and treated with MG132 (10 μM) for the final 2 h. The percentage of cells with misaligned chromosomes is shown. Error bars represent the s.d. (**E**) Quantification of fluorescence intensity (arbitrary unit; AU) of the CENP-E or CENP-F signal at kinetochores in cells expressing GFP-CAMP-Full length or GFP-CAMP-Full length-22A. HeLa cells were treated as in Figure 6D. Misaligned chromosomes in GFP-CAMP-Full length-transfected cells were selected in prometaphase cells. Error bars represent the s.d. (**F**) Recovery of kinetochore levels of CENP-E/CENP-F in cells expressing non-phosphorylatable CAMP mutants. HeLa cells were treated as in Figure 6D. Fluorescence intensity (arbitrary unit; AU) of the CENP-E or CENP-F signal at kinetochores on aligned chromosomes was quantified. Error bars represent the s.d. The results in Figure 6D are schematically shown, as indicated by either '+' or '−'.

segregation (Wong and Fang, 2006; Yokoyama *et al*, 2009). In CAMP-depleted cells, most of the chromosomes aligned on the metaphase plate, but the cells could not maintain chromosome alignment. Similar phenotype was also reported in cells in which RAMA1/Ska3 is depleted (Raaijmakers *et al*, 2009; Theis *et al*, 2009). RAMA1/Ska3 is a component of the Ska complex, which localizes to the spindle and kinetochores (Hanisch *et al*, 2006; Daum *et al*, 2009; Gaitanos *et al*, 2009; Raaijmakers *et al*, 2009; Theis *et al*, 2009; Welburn *et al*, 2009), but in this case it binds directly to microtubules (Welburn *et al*, 2009). The Ska complex is involved in stable kinetochore–microtubule interactions (Gaitanos *et al*, 2009; Raaijmakers *et al*, 2009; Theis *et al*, 2009) and may couple kinetochores with microtubule depolymerization (Welburn *et al*, 2009), as shown previously for the Dam1 complex in budding yeast (Asbury *et al*, 2006; Westermann *et al*, 2006; Tanaka *et al*, 2007). Multipolar spindles in CAMP-depleted cells (Supplementary Figure S3A) probably reflect defective kinetochore–microtubule attachment or defective microtubule organization, resulting indirectly in altered spindle structure, as was observed with Ska1 or RAMA1 depletion (Welburn *et al*, 2009).

CAMP is phosphorylated at serine residues in multiple SPE/D sequences, which reduces its electrophoretic mobility (Figure 6B). We found that mitotic phosphorylation of CAMP is dependent on CDK1 (Figure 6C). It is possible that CDK1, a proline-directed kinase, phosphorylates the SPE/D sequences, although direct phosphorylation of CAMP by CDK1 needs to be proven. Mitotic phosphorylation of CAMP was essential for proper chromosome alignment (Figure 6D). Interestingly, expression of a CAMP mutant with a non-phosphorylatable FPE region did not rescue chromosome misalignment, but phosphorylation became dispensable when CAMP lacked the C-terminal region (Figure 6D). These data suggest that the C-terminal region inhibits the function of the FPE region, and that this inhibition is relieved by serine phosphorylation of the FPE region (Figure 8). One possibility is that the C-terminal region inhibits binding of molecules required for stable kinetochore–microtubule attachment to the FPE region. Alternatively, the C-terminal region binds and thereby masks the FPE region, and this intra-molecular association is counteracted by phosphorylation. As CAMP is conserved only among vertebrates, it is likely to be involved in the fine regulation of chromosome segregation in higher eukaryotes, and dysregulation of its function could be related to oncogenesis.

Materials and methods

Immunofluorescence analysis

Cells grown on coverslips were fixed with acetone/methanol (1:1) for 10 min at room temperature, or with methanol for 10 min (Figure 2C; Supplementary Figures S3B and S7C). For Figures 1B–E and 7A (Supplementary Figures S2A and S7A), cells were pre-permeabilized with 0.1% Triton X-100 for 1 min. Alternatively, cells were fixed with 4% (Supplementary Figures S6A and C and S7B) or 2% (Supplementary Figure S7E) formaldehyde for 15 min at room temperature and permeabilized with 0.2% Triton X-100 for 5 min. For immunofluorescence staining in Figures 3C and E, 4B and C, 7C (Supplementary Figures S3Ai and S6B), cells were fixed with 1% glutaraldehyde for 10 min, as described previously (Savoian *et al*, 1999). Chromosome spreading was performed as described previously (Gimenez-Abian *et al*, 2004). Cells were incubated with primary antibodies overnight at room temperature, followed by incubation with secondary antibodies for 1 h. The secondary antibodies used in this study were goat anti-rabbit IgG Alexa-Fluor-488 and 568, goat anti-mouse Alexa-Fluor-488 and 568, and goat anti-human IgG Alexa-Fluor-568 (Molecular Probes). For antibody dilutions, 0.01% (v/v) Triton X-100 in PBS with 1% BSA (w/v) was used. After a 5-min incubation with 0.1 μg/ml 4′,6-diamidino-2-phenylindole (DAPI), cells were mounted with Fluorescent Mounting Medium (Dako Cytomation). Image stacks were acquired using a Personal DV microscope (Applied Precision) with a ×100 1.40 NA Plan Apochromat oil objective lens (Olympus) mounted on an inverted microscope (CoolSNAP HQ; Photometrics), driven by softWoRx software (Applied Precision, LLC). Z-series image stacks (which were deblurred using softWoRx deconvolution in Figures 3C and E and 4A–C; Supplementary Figure S3Ai) were presented as maximal intensity projections.

Antibodies

The following monoclonal mouse antibodies were used: MAD2L2 (BD Transduction Laboratories), tubulin (B-5-1-2, Sigma), GFP (Roche), CDC27 (BD Transduction Laboratories), BUB1 (14H5, MBL), BUBR1 (8G1, MBL), CENP-E (1H12, Abcam), HEC1 (9G3, Abcam), Flag (M2, Sigma), His (GE Healthcare), γ-tubulin (GTU-88, Sigma), MPS1 (Abcam), CENP-C (Santa Cruz Biotechnology), Aurora B (BD Transduction Laboratories), RanBP2 (Santa Cruz Biotechnology), and EB1 (BD Transduction Laboratories). A mouse polyclonal antibody against CAMP (C13orf8, Abnova) was used for immunostaining. The following polyclonal rabbit antibodies were used: CAMP (C13orf8, Sigma), MAD2L1 (Novus Biologicals), CENP-E (Sigma), CENP-F (Abcam), Blinkin (Novus Biologicals), RanGAP1 (Santa Cruz Biotechnology), CLIP-170 (Santa Cruz Biotechnology), ch-TOG (Abcam), phospho-histone H3 Ser10 (Cell Signaling Technologies), and KID (Cytoskeleton). Rabbit polyclonal anti-HP1α, CAP-G (Nakajima *et al*, 2007), and CAP-G2 antibodies were raised against polypeptides based on the respective proteins. We also used a human auto-antibody against centromeric antigens (CREST serum; Nakajima *et al*, 2007), a goat polyclonal anti-actin antibody (Santa Cruz Biotechnology), and a rabbit monoclonal anti-phospho-histone H3 Thr3 antibody (Upstate Biotechnology).

siRNAs

The targeted CAMP sequences were as follows: oligo 1, 5′-CCGGCAUAAUGAAGAGGCAAAUAAA-3′, oligo 2, 5′-GGAAACACAGAAACUUGGUUCAGUU-3′ (Stealth, Invitrogen). The targeted sequences for MAD2L1, MAD2L2, MPS1, BUB1, BUBR1, CENP-E, and CENP-F were 5′-AGAAUUGGUAAUAAACUGUGGUCCC-3′, 5′-AAAGACGAAUUUCUCCACUGGGCGG-3′, 5′-UUUGAAAGUAGUCACGUGCAUCAUC-3′, 5′-UUUGAAGGAAGUCUGCUGACAGAGC-3′, 5′-UUUACAUGGUGUCAUAACUGGCUGU-3′, 5′-UUUAAGUUCCUCUUCAGUUUCCAGG-3′, and 5′-AGAAUUAGAUGAAAGAUGACUUGGG-3′, respectively (Stealth, Invitrogen).

Live-cell imaging

HeLa cells were grown in chambered coverslips (Laboratory-Tek; Thermo Fisher Scientific). One hour before imaging, the medium was changed to pre-warmed Leibovitz's L-15 medium, and the chamber lids were sealed with silicone grease. Recordings were made at 37°C using a temperature-controlled incubator. Time-lapse images were collected using a Personal DV microscope. For the experiment in Figure 4A, cells expressing EGFP-CENP-A and EGFP-α-tubulin were flattened by the pressure of the agar overlay. A piece of 3% agar gel was placed on the cells in the chambered coverslip and the medium was removed to press the cells to around half the original thickness (~10 μm) before imaging.

Supplementary data

Supplementary data are available at *The EMBO Journal* Online (http://www.embojournal.org).

Acknowledgements

We thank J-M Peters for EGFP-CENP-A/EGFP-α-tubulin cell; A Harata, T Aizawa, S Arai, and S Shimanuki for technical assistance; and TU Tanaka, M Satake, and T Shiraki for helpful discussions. This work was supported by Special Coordination Funds for Promoting Science and Technology from the Japan Science and Technology Agency; a Grant-in-Aid for Scientific Research from the Japanese Society of Promotion of Science; a Grant-in-Aid for

Scientific Research from the Ministry of Education, Culture, Sports, Science and Technology of Japan; a grant from the Tohoku University 'Evolution' program; and grants from the Naito Foundation, the NOVARTIS Foundation, and the Takeda Science Foundation.

Author contributions: SK carried out the far western analysis, KSKU contributed to the live-cell imaging, SC, SS, KW, and KM were involved in the biochemical experiments, and AY contributed to the MS work. GI performed all other experiments. TH and KT supervised research and wrote the paper.

Conflict of interest

The authors declare that they have no conflict of interest.

References

Asbury CL, Gestaut DR, Powers AF, Franck AD, Davis TN (2006) The Dam1 kinetochore complex harnesses microtubule dynamics to produce force and movement. *Proc Natl Acad Sci USA* **103:** 9873–9878

Ashar HR, James L, Gray K, Carr D, Black S, Armstrong L, Bishop WR, Kirschmeier P (2000) Farnesyl transferase inhibitors block the farnesylation of CENP-E and CENP-F and alter the association of CENP-E with the microtubules. *J Biol Chem* **275:** 30451–30457

Baker DJ, Dawlaty MM, Galardy P, van Deursen JM (2007) Mitotic regulation of the anaphase-promoting complex. *Cell Mol Life Sci* **64:** 589–600

Bomont P, Maddox P, Shah JV, Desai AB, Cleveland DW (2005) Unstable microtubule capture at kinetochores depleted of the centromere-associated protein CENP-F. *EMBO J* **24:** 3927–3939

Cahill DP, da Costa LT, Carson-Walter EB, Kinzler KW, Vogelstein B, Lengauer C (1999) Characterization of MAD2B and other mitotic spindle checkpoint genes. *Genomics* **58:** 181–187

Cassimeris L, Morabito J (2004) TOGp, the human homolog of XMAP215/Dis1, is required for centrosome integrity, spindle pole organization, and bipolar spindle assembly. *Mol Biol Cell* **15:** 1580–1590

Chan GK, Schaar BT, Yen TJ (1998) Characterization of the kinetochore binding domain of CENP-E reveals interactions with the kinetochore proteins CENP-F and hBUBR1. *J Cell Biol* **143:** 49–63

Cheeseman IM, Chappie JS, Wilson-Kubalek EM, Desai A (2006) The conserved KMN network constitutes the core microtubule-binding site of the kinetochore. *Cell* **127:** 983–997

Cheeseman IM, Desai A (2008) Molecular architecture of the kinetochore-microtubule interface. *Nat Rev Mol Cell Biol* **9:** 33–46

Chen J, Fang G (2001) MAD2B is an inhibitor of the anaphase-promoting complex. *Genes Dev* **15:** 1765–1770

Cheung HW, Chun AC, Wang Q, Deng W, Hu L, Guan XY, Nicholls JM, Ling MT, Chuan Wong Y, Tsao SW, Jin DY, Wang X (2006) Inactivation of human MAD2B in nasopharyngeal carcinoma cells leads to chemosensitization to DNA-damaging agents. *Cancer Res* **66:** 4357–4367

Dai J, Sultan S, Taylor SS, Higgins JM (2005) The kinase haspin is required for mitotic histone H3 Thr 3 phosphorylation and normal metaphase chromosome alignment. *Genes Dev* **19:** 472–488

Daum JR, Wren JD, Daniel JJ, Sivakumar S, McAvoy JN, Potapova TA, Gorbsky GJ (2009) Ska3 is required for spindle checkpoint silencing and the maintenance of chromosome cohesion in mitosis. *Curr Biol* **19:** 1467–1472

De Luca M, Brunetto L, Asteriti IA, Giubettini M, Lavia P, Guarguaglini G (2008) Aurora-A and ch-TOG act in a common pathway in control of spindle pole integrity. *Oncogene* **27:** 6539–6549

Draviam VM, Shapiro I, Aldridge B, Sorger PK (2006) Misorientation and reduced stretching of aligned sister kinetochores promote chromosome missegregation in EB1- or APC-depleted cells. *EMBO J* **25:** 2814–2827

Dyson HJ, Wright PE (2005) Intrinsically unstructured proteins and their functions. *Nat Rev Mol Cell Biol* **6:** 197–208

Feng J, Huang H, Yen TJ (2006) CENP-F is a novel microtubule-binding protein that is essential for kinetochore attachments and affects the duration of the mitotic checkpoint delay. *Chromosoma* **115:** 320–329

Gaitanos TN, Santamaria A, Jeyaprakash AA, Wang B, Conti E, Nigg EA (2009) Stable kinetochore-microtubule interactions depend on the Ska complex and its new component Ska3/C13Orf3. *EMBO J* **28:** 1442–1452

Gan GN, Wittschieben JP, Wittschieben BO, Wood RD (2008) DNA polymerase zeta (pol zeta) in higher eukaryotes. *Cell Res* **18:** 174–183

Ganem NJ, Storchova Z, Pellman D (2007) Tetraploidy, aneuploidy and cancer. *Curr Opin Genet Dev* **17:** 157–162

Gimenez-Abian JF, Sumara I, Hirota T, Hauf S, Gerlich D, de la Torre C, Ellenberg J, Peters JM (2004) Regulation of sister chromatid cohesion between chromosome arms. *Curr Biol* **14:** 1187–1193

Green RA, Wollman R, Kaplan KB (2005) APC and EB1 function together in mitosis to regulate spindle dynamics and chromosome alignment. *Mol Biol Cell* **16:** 4609–4622

Hanisch A, Sillje HH, Nigg EA (2006) Timely anaphase onset requires a novel spindle and kinetochore complex comprising Ska1 and Ska2. *EMBO J* **25:** 5504–5515

Hoffman DB, Pearson CG, Yen TJ, Howell BJ, Salmon ED (2001) Microtubule-dependent changes in assembly of microtubule motor proteins and mitotic spindle checkpoint proteins at PtK1 kinetochores. *Mol Biol Cell* **12:** 1995–2009

Holt SV, Vergnolle MA, Hussein D, Wozniak MJ, Allan VJ, Taylor SS (2005) Silencing Cenp-F weakens centromeric cohesion, prevents chromosome alignment and activates the spindle checkpoint. *J Cell Sci* **118:** 4889–4900

Howell BJ, Moree B, Farrar EM, Stewart S, Fang G, Salmon ED (2004) Spindle checkpoint protein dynamics at kinetochores in living cells. *Curr Biol* **14:** 953–964

Hussein D, Taylor SS (2002) Farnesylation of Cenp-F is required for G2/M progression and degradation after mitosis. *J Cell Sci* **115:** 3403–3414

Iakoucheva LM, Radivojac P, Brown CJ, O'Connor TR, Sikes JG, Obradovic Z, Dunker AK (2004) The importance of intrinsic disorder for protein phosphorylation. *Nucleic Acids Res* **32:** 1037–1049

Ishida T, Kinoshita K (2007) PrDOS: prediction of disordered protein regions from amino acid sequence. *Nucleic Acids Res* **35:** W460–W464

Iwai H, Kim M, Yoshikawa Y, Ashida H, Ogawa M, Fujita Y, Muller D, Kirikae T, Jackson PK, Kotani S, Sasakawa C (2007) A bacterial effector targets Mad2L2, an APC inhibitor, to modulate host cell cycling. *Cell* **130:** 611–623

Johnson VL, Scott MI, Holt SV, Hussein D, Taylor SS (2004) Bub1 is required for kinetochore localization of BubR1, Cenp-E, Cenp-F and Mad2, and chromosome congression. *J Cell Sci* **117:** 1577–1589

Khodjakov A, Copenagle L, Gordon MB, Compton DA, Kapoor TM (2003) Minus-end capture of preformed kinetochore fibers contributes to spindle morphogenesis. *J Cell Biol* **160:** 671–683

Kiyomitsu T, Iwasaki O, Obuse C, Yanagida M (2010) Inner centromere formation requires hMis14, a trident kinetochore protein that specifically recruits HP1 to human chromosomes. *J Cell Biol* **188:** 791–807

Laoukili J, Kooistra MR, Bras A, Kauw J, Kerkhoven RM, Morrison A, Clevers H, Medema RH (2005) FoxM1 is required for execution of the mitotic programme and chromosome stability. *Nat Cell Biol* **7:** 126–136

Lawo S, Bashkurov M, Mullin M, Ferreria MG, Kittler R, Habermann B, Tagliaferro A, Poser I, Hutchins JR, Hegemann B, Pinchev D, Buchholz F, Peters JM, Hyman AA, Gingras AC, Pelletier L (2009) HAUS, the 8-subunit human Augmin complex, regulates centrosome and spindle integrity. *Curr Biol* **19:** 816–826

Liu D, Ding X, Du J, Cai X, Huang Y, Ward T, Shaw A, Yang Y, Hu R, Jin C, Yao X (2007) Human NUF2 interacts with centromere-associated protein E and is essential for a stable spindle microtubule-kinetochore attachment. *J Biol Chem* **282:** 21415–21424

Maiato H, Rieder CL, Khodjakov A (2004) Kinetochore-driven formation of kinetochore fibers contributes to spindle assembly during animal mitosis. *J Cell Biol* **167:** 831–840

McEwen BF, Chan GK, Zubrowski B, Savoian MS, Sauer MT, Yen TJ (2001) CENP-E is essential for reliable bioriented spindle attachment,

but chromosome alignment can be achieved via redundant mechanisms in mammalian cells. *Mol Biol Cell* **12:** 2776–2789

Medendorp K, van Groningen JJ, Vreede L, Hetterschijt L, van den Hurk WH, de Bruijn DR, Brugmans L, van Kessel AG (2009) The mitotic arrest deficient protein MAD2B interacts with the small GTPase RAN throughout the cell cycle. *PLoS One* **4:** e7020

Musacchio A, Salmon ED (2007) The spindle-assembly checkpoint in space and time. *Nat Rev Mol Cell Biol* **8:** 379–393

Nakajima M, Kumada K, Hatakeyama K, Noda T, Peters JM, Hirota T (2007) The complete removal of cohesin from chromosome arms depends on separase. *J Cell Sci* **120:** 4188–4196

Okada T, Sonoda E, Yoshimura M, Kawano Y, Saya H, Kohzaki M, Takeda S (2005) Multiple roles of vertebrate REV genes in DNA repair and recombination. *Mol Cell Biol* **25:** 6103–6111

Pfleger CM, Salic A, Lee E, Kirschner MW (2001) Inhibition of Cdh1-APC by the MAD2-related protein MAD2L2: a novel mechanism for regulating Cdh1. *Genes Dev* **15:** 1759–1764

Putkey FR, Cramer T, Morphew MK, Silk AD, Johnson RS, McIntosh JR, Cleveland DW (2002) Unstable kinetochore-microtubule capture and chromosomal instability following deletion of CENP-E. *Dev Cell* **3:** 351–365

Raaijmakers JA, Tanenbaum ME, Maia AF, Medema RH (2009) RAMA1 is a novel kinetochore protein involved in kinetochore-microtubule attachment. *J Cell Sci* **122:** 2436–2445

Ricke RM, van Ree JH, van Deursen JM (2008) Whole chromosome instability and cancer: a complex relationship. *Trends Genet* **24:** 457–466

Ruchaud S, Carmena M, Earnshaw WC (2007) Chromosomal passengers: conducting cell division. *Nat Rev Mol Cell Biol* **8:** 798–812

Savoian MS, Earnshaw WC, Khodjakov A, Rieder CL (1999) Cleavage furrows formed between centrosomes lacking an intervening spindle and chromosomes contain microtubule bundles, INCENP, and CHO1 but not CENP-E. *Mol Biol Cell* **10:** 297–311

Schaar BT, Chan GK, Maddox P, Salmon ED, Yen TJ (1997) CENP-E function at kinetochores is essential for chromosome alignment. *J Cell Biol* **139:** 1373–1382

Schafer-Hales K, Iaconelli J, Snyder JP, Prussia A, Nettles JH, El-Naggar A, Khuri FR, Giannakakou P, Marcus AI (2007) Farnesyl transferase inhibitors impair chromosomal maintenance in cell lines and human tumors by compromising CENP-E and CENP-F function. *Mol Cancer Ther* **6:** 1317–1328

Tanaka K, Hirota T (2009) Chromosome segregation machinery and cancer. *Cancer Sci* **100:** 1158–1165

Tanaka K, Kitamura E, Kitamura Y, Tanaka TU (2007) Molecular mechanisms of microtubule-dependent kinetochore transport toward spindle poles. *J Cell Biol* **178:** 269–281

Tanaka TU (2008) Bi-orienting chromosomes: acrobatics on the mitotic spindle. *Chromosoma* **117:** 521–533

Tanaka TU, Desai A (2008) Kinetochore-microtubule interactions: the means to the end. *Curr Opin Cell Biol* **20:** 53–63

Tanaka TU, Stark MJ, Tanaka K (2005) Kinetochore capture and bi-orientation on the mitotic spindle. *Nat Rev Mol Cell Biol* **6:** 929–942

Tanenbaum ME, Galjart N, van Vugt MA, Medema RH (2006) CLIP-170 facilitates the formation of kinetochore-microtubule attachments. *EMBO J* **25:** 45–57

Theis M, Slabicki M, Junqueira M, Paszkowski-Rogacz M, Sontheimer J, Kittler R, Heninger AK, Glatter T, Kruusmaa K, Poser I, Hyman AA, Pisabarro MT, Gstaiger M, Aebersold R, Shevchenko A, Buchholz F (2009) Comparative profiling identifies C13orf3 as a component of the Ska complex required for mammalian cell division. *EMBO J* **28:** 1453–1465

Tokai-Nishizumi N, Ohsugi M, Suzuki E, Yamamoto T (2005) The chromokinesin Kid is required for maintenance of proper metaphase spindle size. *Mol Biol Cell* **16:** 5455–5463

Tulu US, Fagerstrom C, Ferenz NP, Wadsworth P (2006) Molecular requirements for kinetochore-associated microtubule formation in mammalian cells. *Curr Biol* **16:** 536–541

Uehara R, Nozawa RS, Tomioka A, Petry S, Vale RD, Obuse C, Goshima G (2009) The augmin complex plays a critical role in spindle microtubule generation for mitotic progression and cytokinesis in human cells. *Proc Natl Acad Sci USA* **106:** 6998–7003

Vergnolle MA, Taylor SS (2007) Cenp-F links kinetochores to Ndel1/Nde1/Lis1/dynein microtubule motor complexes. *Curr Biol* **17:** 1173–1179

Walczak CE, Cai S, Khodjakov A (2010) Mechanisms of chromosome behaviour during mitosis. *Nat Rev Mol Cell Biol* **11:** 91–102

Weaver BA, Cleveland DW (2005) Decoding the links between mitosis, cancer, and chemotherapy: The mitotic checkpoint, adaptation, and cell death. *Cancer Cell* **8:** 7–12

Welburn JP, Grishchuk EL, Backer CB, Wilson-Kubalek EM, Yates III JR, Cheeseman IM (2009) The human kinetochore Ska1 complex facilitates microtubule depolymerization-coupled motility. *Dev Cell* **16:** 374–385

Westermann S, Wang HW, Avila-Sakar A, Drubin DG, Nogales E, Barnes G (2006) The Dam1 kinetochore ring complex moves processively on depolymerizing microtubule ends. *Nature* **440:** 565–569

Wong J, Fang G (2006) HURP controls spindle dynamics to promote proper interkinetochore tension and efficient kinetochore capture. *J Cell Biol* **173:** 879–891

Yang Z, Guo J, Chen Q, Ding C, Du J, Zhu X (2005) Silencing mitosin induces misaligned chromosomes, premature chromosome decondensation before anaphase onset, and mitotic cell death. *Mol Cell Biol* **25:** 4062–4074

Yao X, Abrieu A, Zheng Y, Sullivan KF, Cleveland DW (2000) CENP-E forms a link between attachment of spindle microtubules to kinetochores and the mitotic checkpoint. *Nat Cell Biol* **2:** 484–491

Yokoyama H, Rybina S, Santarella-Mellwig R, Mattaj IW, Karsenti E (2009) ISWI is a RanGTP-dependent MAP required for chromosome segregation. *J Cell Biol* **187:** 813–829

Zhang XD, Goeres J, Zhang H, Yen TJ, Porter AC, Matunis MJ (2008) SUMO-2/3 modification and binding regulate the association of CENP-E with kinetochores and progression through mitosis. *Mol Cell* **29:** 729–741

